Adv Polym Sci (2021) 287: 343–360
https://doi.org/10.1007/12_2021_83

Published online: 21 May 2021

# Chitosan–Stem Cell Interactions


**Lalitha Sarad Yamini Nanduri**

## Contents



**Abstract** Chitosan, the deacetylated form of chitin, has been extensively used for tissue engineering in the form of hydrogel, scaffolds, microparticles, nanoparticles, and nanofibers. To develop composite constructs with targeted tissue regeneration, chitosan is often combined with hydroxyapatite, collagen, gelatin, hyaluronic acid, silk fibroin, etc. biomaterials. In addition to this, chitosan is often modified with varied physico-chemical properties. For regenerative application, to improve the efficacy of constructs, chitosan in various forms is combined with various stem cells, among which mesenchymal stem cells (MSCs) have been studied widely. In this review we focused on the studies that exclusively used chitosan in combination with multipotent adipose and bone marrow-derived MSCs and pluripotent-induced pluripotent stem cells (iPSCs). When cultured on chitosan, stem cells displayed greater affinity in terms of cellular adhesion, proliferation, and differentiation into functional cell types both in vitro albeit different potential. When transplanted in vivo, stem cell-laden chitosan constructs showed greater integrity into the host system, differentiated into targeted cells, and demonstrated improved repair of the damaged tissue. These studies provide great insight into the current and future potential of chitosan for regenerative applications.

L. S. Y. Nanduri (✉)
Department of Radiation Oncology, Albert Einstein College of Medicine, Bronx, NY, USA

**Keywords** Cell-laden constructs · Chitosan–stem cell interaction · Exosomes · Stem cells

## 1 Introduction

Chitin is a polysaccharide obtained from the coat of the crustaceans. Various form of chitin has been generated by chemical and physical modifications. Chitosan (CS) is one such form generated by deacetylation of chitin [1–5]. The degree of deacetylation has an influence on its properties [6]. CS is mainly composed of D-glucosamine and N-acetyl-D-glucosamine that are linked randomly with β-1,4-linkage. These components in CS interact with the extracellular matrix components and modulate regenerative signals. Till date CS has been widely investigated in the form of hydrogels, scaffolds, nanoparticles, nanotubes. Depending on the application chitosan is used either alone or in combination with other biomaterials such as chitin, hyaluronic acid, hydroxyapatite (HA), collagen, silk fibroin, agarose, and/or not limited to graphene [2, 3, 7] (Fig. 1). For instance, CS in combination with HA is tested widely for bone regeneration. CS is biodegradable, biocompatible, anti-microbial [8, 9], and non-toxic which makes it an interesting biomaterial of choice for various regenerative [10, 11] biological applications. In addition to tissue regeneration, CS has been tested for anti-microbial [12] drug delivery [13]. CS has been tested for wound healing [4, 14–16], bone regeneration [17], neuronal regeneration [7], soft tissue regeneration [18], epithelial branching morphogenesis [19], skin regeneration [20–22], and with intestinal epithelial cells [23, 24].

Stem cells (SCs) are known as the rare and undifferentiated cells of a tissue with unique potential to self-renew and differentiate into functional cells. For instance, in healthy tissues, loss of functional cells is balanced by the addition of new cells by resident SCs of the tissue. SCs self-renew to maintain their own number to be

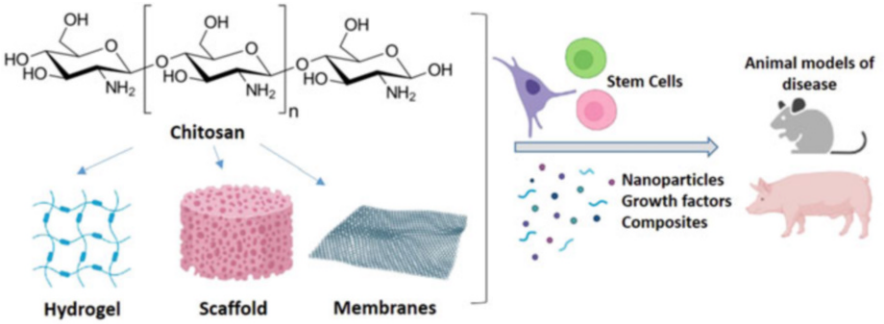


**Fig. 1** Schematic showing different forms and applications of chitosan. Made with Biorender.com

supportive for tissue homeostasis for years to come. However, factors such as aging or irreversible tissue damage might diminish the number and potential of stem cells, which eventually leads to loss of tissue functionality. Based on their origin, stem cells are divided into two categories, adult SCs are obtained from adult tissues and embryonic SCs are obtained from fetal tissues; another category is the induced pluripotent SCs (iPSCs)-developed in in vitro. Adult and iPSCs are widely investigated for regenerative application. Various adult SCs, such as mesenchymal stem cells (MSCs) derived from adipose (AD-MSCs), bone marrow (BM-MSCs), and umbilical cord blood (UC-MSCs) and to some extent iPSCs were studied for their interaction with the biomaterial—chitosan.

Either injectable hydrogels, scaffolds, or grafts, the success of tissue engineering constructs depends mostly on the biomaterial of choice and cell type. The main expectation of the biomaterial to be used is to be non-toxic and support the growth of cells in vitro and in vivo. Various factors such as chemistry of components, pore size, stiffness, stability etc. are known to influence the interaction between biomaterial and cells. Therefore, to develop successful tissue engineering strategies, it is a prerequisite to understand how a biomaterial such as CS interacts with various types of cells. In this review, we focused on reports from literature that have investigated the potential of different SCs to interact with chitosan and interesting findings thereof. In the interest of regenerative application, we have focused here mainly on the interaction of various stem cells with chitosan.

## 2 Chitosan–Stem Cell Interactions

Mesenchymal stem or stromal cells popularly known as “medicinal signaling cells” have been widely investigated for regenerative applications for various diseases including the most recent COVID-19. According to the guidelines of International Society of Cell and Gene Therapy, MSCs are defined to express CD73, CD90, and CD105 on surface and possess multi-lineage differentiation into osteocytes, chondrocytes, and adipocytes [25]. In addition to the multi-lineage differentiation potential, MSCs are known to be immunomodulatory and regenerative. However, based on their source of origin, adipose, bone marrow, or cord blood, the MSCs possess distinct differentiation and regenerative potential [26].

### *2.1 Bone Marrow-Derived MSCs*

Midha et al. [27] have tested the osteogenesis potential of BM-MSCs, using a highly porous, multi-material composite made of chitosan/hydroxyapatite/polycaprolactone (CHT/HA/PCL) in 3:3:2 (wt/vol). They observed that 21-day post-culture of $5 \times 10^4$ cells/composite, AD-MSCs<BM-MSCs<WJ-MSCs showed an increasing cellular activity with WJ-MSCs showing maximal activity.

When subjected to osteogenic differentiation on the composites, BM-MSCs showed significant fibroblastic cellular morphology at day 7, stellate-shaped at day 14, and showed mineralization at day 21 (increased *OCN* expression), when compared to AD-MSCs and WJ-MSCs, indicative of their successful cell–matrix interaction. In addition, BM-MSCs showed a two times increase in mRNA level expression of *Col I* expression, protein level (immunostaining) expression of COL I at day 7, β-CATENIN, OCN etc. in comparison to AD-MSCs on the composites. Composites were cultured for 7 days with undifferentiated BM-MSCs and implanted into rats with 3 mm load-bearing defect and followed over time using micro-CT and histology, acellular constructs were control. In addition to complete integration of composites at 6-week post-implant, BM-MSC laden composites showed improved bone regeneration, 21% increase in trabecular BV/TV compared to 16% in acellular composites. HE, Masson trichome staining of the bone confirmed the neobone formation in rats implanted with BM-MSC laden composites. This study concluded that in vitro screening has identified a better choice of BM-MSCs for osseointegration in vivo which resulted in improved integration and neobone formation in the bone defect model.

Yan et al. [28] have investigated the BM-MSC laden collagen–chitosan scaffold for the recovery of neuropathological injury using traumatic brain injury (TBI) model. Collagen/chitosan scaffolds of 3 × 3 × 2 mm with 80–200 μm pore size were prepared and cultured with $2 \times 10^6$/μL of (rat BM-MSCs) for 48 h. TBI was made in rats with a 10 mm diameter craniotomy adjacent to the sagittal suture and midway between lambda and bregma, and 72 h post-TBI, cell-laden scaffolds were transplanted in situ into the injured area. TBI with BM-MSC laden scaffold with and without immunosuppressor and TBI + BMSCs stereotactic injection without the scaffold and TBI without transplant were the control groups. Modified Neurological Severity Scores (mNSS) on day 1 and day 7 were significantly declined in all groups especially those with BMSC-scaffold, when compared to TBI only control. Average frequency of crossing the platform (Morris water maze test) showed a significant reduction in the transplanted groups indicative of recovery, in comparison to TBI only control up to days 35 post-transplant. Also, average escape latency (Morris water maze test) was improved in BMSC-scaffold and BMSC alone groups, compared to TBI only control. Histological evaluation post-30 days showed more GFAP positive BrU-labeled BM-MSCs at day 7 and day 14. This study concluded that BM-MSCs accelerated the functional recovery of rats after transplant.

As an alternate to cell-laden constructs, Wang et al. [29] investigated the potential of magnetic lanthanum-doped hydroxyapatite/chitosan (MLaHA/CS) scaffolds to facilitate endogenous stem cell recruitment for bone regeneration. They have used freeze-drying method to generate CS scaffolds with $SrFe_{12}O_{19}$ nanoparticles, $Ca^{+2}$, $La^{3+}$, and $PO_4^{3-}$ ions, and nanorod bundles of LaHA were deposited on the surface and characterized for their pore size, hydrophilicity, magnetic, thermal, ion release, mechanical and biocompatible properties. They observed that when $1 \times 10^4$ rat BM-MSCs seeded/scaffold, MLaHA/CS showed higher viability (CCK-8 assay) and attracted more BM-MSCs (cell migration assay) when compared to LaHA/CS than HA/CS scaffolds. When tested for anti-inflammatory property with RAW264.7

macrophages, MLaHA/CS showed less M1 more number of M2 (CD206), anti-inflammatory and pro-regenerative macrophages in comparison to controls. In addition, MLaHA/CS showed higher osteogenic induction as indicated by increase in mRNA levels of ALP, BMP-2, OCN, RUNX-2, and activation of p-smad pathway in comparison to HA/CS and LaHA/CS scaffolds. To test the in vivo bone regenerative potential, 5 × 2 mm scaffolds were prepared and implanted into transosseous defect in the cranium of rats, calcein and alizarin red were injected 4- and 6-week post-implantation to detect the neobone formation. Micro-CT data 12-week post-implant showed new bone formation, higher BV/TV%, higher TBNs and TBTs with MLaHA/CS scaffolds. Calcitonin, alizarin red staining in the implant area was more and showed significantly enhanced generation of newly formed and mineralized bone in MLaHA/CS implant groups at 4 and 8 weeks, respectively, when compared to controls. At 12-week post-implantation, more M2 polarization was detected in MLaHA/CS scaffold group, together confirming overall improved bone regeneration with MLaHA/CS scaffolds when compared to HA/CS and LaHA/CS scaffolds.

Liu et al. [30] have studied the potential of BM-MSC incorporated, thermosensitive chitosan hydrogel to repair myocardial infarction in mice. BM-MSCs expressing Fluc and GFP were isolated from transgenic mice and $1 \times 10^4$ cells/well were seeded together with different concentrations of CS hydrogel (0.5–2 mg/mL) and found that 1 mg/mL of CS hydrogel showed an optimal proliferation of BM-MSCs based on CCK8 assay and mRNA expression of epidermal (EGF), platelet-derived (PGF), hepatocyte (HGF), and insulin (IGF) growth factors. After induction of myocardial infarction in mice, $2 \times 10^5$ BMSCs/20 μL CS hydrogel (1 mg/mL) was transplanted with 30-gauge needle into 2 position adjacent to the infarcted area, PBS was injected as control. In 30-day post-transplant echocardiography, left ventricle (LV) showed significant enlargement, anterior and posterior walls of LV were thinned. BM-MSC/CS hydrogel recipients showed a significant decrease in LVIDd and LVIDs of hearts after infarction, maintained LV contractile function with increases in FS and EF in comparison to CS only and PBS controls. CD31 (endothelial cell marker) staining at day 30 showed a significant increase in capillary density in the border region. In addition, day 5 post-transplant, a significant reduction in IL-6, TNF-a, IL-1b, IL-18, caspase-11, and caspase-1 was observed in BM-MSC/CS group, then in BM-MSC alone group and PBS only treated group. BM-MSC/CS group showed relatively less expression of caspase-1 in vascular endothelial cells ($CD31^+$) compared to the controls, indicating a reduction in pyroptosis in BM-MSC treated group. When LPS and ATP treated human umbilical vein endothelial cells (HUVECs) were treated with the conditioned media of BM-MSC/CS, they observed survival of HUVECs and decrease in pyroptosis related genes caspasae-1 and GSDMD, in comparison to the BMSCs alone controls. This study concluded the promising cardiac regenerative potential of CS hydrogel when incorporated with BM-MSCs.

## 2.2 Adipose-Derived MSCs (AD-MSCs)

Altman et al. [31] have investigated the effect of 75:25 silk fibroin:chitosan blend scaffold (SFCS) on seeding and in vivo delivery of human adipose-derived SCs (hASCs) on wound healing. hASCs between passages 1–8 either alone or were transfected with lentiviral eGFP and $1 \times 10^5$ cells were seeded/cm$^2$ of the SFCS scaffold and cultured for 24–48 h, washed with PBS and sutured into 6 mm diameter cutaneous wound, and followed for 0–10 days. Planimetric analysis on day 8 post-transplantation revealed a wound closure of 55 ± 17% in control without graft, 75 ± 11% in acellular-SFCS group and 90 ± 3% in ASC-SFCS group and by day 14 they observed a complete epithelialization in ASC-SFCS treated group. Post-2 weeks, microvascular density of wound bed biopsy specimen showed an increase in 7.5 ± 1.1 vessels/high power field in ASC-SFCS group, compared to 5.1 ± 1.0 vessels/high power field in acellular-SFCS group. At 2 weeks post, GFP$^+$ cells were observed in the dermis and cutaneous appendages and were positive for Ki67, SMA, vascular smooth muscle marker and HSP-47. At 4 weeks post, GFP$^+$ cells co-stained with cytokeratin19 (CK19) and no GFP$^+$ cells were observed 4 cm away from the site of graft. This study concluded that SFCS can support migration, proliferation, and differentiation of the seeded cells.

Liu et al. [32] have tested the rat AD-MSCs in an injectable chitosan hydrogel system to improve myocardial infarction (MI). Improper angiogenesis, inflammation, reactive oxygen species (ROS) in the MI microenvironment make it very hostile for the regenerative stem cells to home. Therefore, first they studied the role of components in CS to rescue the impaired cellular adhesion of AD-MSCs, against ROS in vitro. When seeded on culture plates, 30 μM $H_2O_2$ inhibited the adhesion of AD-MSCs to 63.6 ± 1.37%, which was improved to 89 ± 4.32% and 88.3 ± 4.97%, when treated with 0.5 mg/mL pf N-AC-Glu and D-Glu, the components of CS, respectively. RT-PCR data showed that ROS treatment reduced the mRNA level of integrin β1 and αV, decreased phosphorylation of FAK, Src, and p-AKt, and increased cleaved-caspase3, which were significantly restored when treated with N-AC-Glu and D-Glu. Further luciferase labeled $4 \times 10^6$ AD-MSCs in 100 μL CS hydrogel (ADSC/CS) were injected along the border of infract areas with 28-guage needle in male SD-rats and ADSC/PBS was injected as control in infract hearts. Bioluminescence imaging (BLI) at day 7 and day 14 showed a two- and four-time increase, respectively, in ADSC/Chitosan compared to ADSC/PBS, indicating cellular retention, whereas at day 28, no signal observed in ADSC/PBS whereas significant signals remained in ADSC/chitosan group, indicating retention, engraftment, and survival of ADSCs. Echocardiography data at 4 weeks showed an improved left ventricular fractional shorting (LVFS) and increased 52.92 ± 5.76% left ventricular ejection fraction (LVEF) when compared to PBS control (42.64 ± 3.8%). In addition, ADSC/chitosan treated rats showed improved hemodynamics, relatively decreased post-ischemic apoptosis (TUNEL staining), reduced infarct size, and improved arteriole density when compared to PBS control. Further the histological analysis showed luciferase-ADSCs co-staining with cTnT and

a-Sarcomeric actin, whereas some ADSCs were positive for vWAg and CD31, vascular markers, indicating differentiation of transplanted ADSCs.

Cheng et al. [33] have shown improved spheroid formation, upregulation of pluripotency genes, and increased transdifferentiation efficiency of human AD-MSCs (hASCs). Time-lapse live cell imaging showed that ASCs were motile and readily aggregated on CS coated plates and showed increase in spheroid formation with increase in cell densities from $1.5 \times 10^3$ to $5 \times 10^4$ cells/cm$^2$, which did not compromise cell viability when compared to cells in monolayer. ASCs in spheroids showed decrease in expression of CD29, CD90, CD105 and increase in expression of CD34, CD44, and PECAM, reduced apoptosis, increase in fibronectin, laminin when compared to those in monolayer. Quantification of mRNA levels showed a 7.7, 4.9, and 2.9 fold increase in expression of pluripotent markers Sox-2, Oct-4, and Nanog in ASC spheroids on day 3 compared to that at day 0, similar increase was observed at day 7 ASC-spheroids. When seeded back to tissue culture plates without coating, ASC-spheroids spread and show a 2.5-fold increase in activity index at day 3, a 3.2-fold and 2.7-fold increase in activity index at day 5 and day 7, respectively. When ASC spheroids were trypsinized, the single cells obtained were cultured for 14 days and showed increase in number of $71.3 \pm 2.5$ colony forming units (CFU), whereas monolayer derived ASCs showed $30.6 \pm 8.1$ CFUs. RT-PCR data showed a significant improvement in osteogenic induction (Runx2) of ASC-spheroids when compared to monolayer cells; however, no such difference observed with adipogenic induction (PPAR-γ). In addition, they observed increase in mRNA and protein levels of Nestin and albumin in ASC spheroids when cultured for 14 days in neurogenic and hepatogenic media. When dissociated and intra-muscularly transplanted into hind limbs of nude mice, ASC-spheroids showed more HNA-positive cells/injection group at day 7 and day 21 post-transplant. This data indicated a non-chemical based activation of AD-MSCs, using chitosan which improved sphere formation, stem cell marker expression, transdifferentiation in vitro and better cellular retention post-intramuscular injection in vivo.

Liu et al. [34] have isolated stromal vesicular fraction (SVF) from 9-day-old piglets and obtained AD-MSCs (pADSCs) that expressed CD29, CD44, and MHC I and negative for CD31, CD45, and MHC II and were able to differentiate into adipo, osteo, and chondrocytes. pADSCs were cultured on 1% chitosan coated tissue culture plate and differentiated into pancreatic islet-like clusters (PILC). Immunostaining data showed increased production of β-cell signature markers Pdx-1, ISL-2 and insulin was relatively more in CS coated plates at day 3. RT-PCR data showed that CS increased β-cell development gene, Pax4 and also for Pdx-1, glucokinase and insulin and maintained the expression of Glut2, Pdx-1 from day 6–day 15, whereas these levels not maintained in the absence of CS. When supplemented with 5.5 mM to 25 mM doses of glucose, increased secretion of insulin 1.0 ng/μg of protein and 1.5 ng/μg of protein was observed in the presence of CS at day 9 and day 15 to 25 mM glucose concentration, respectively. Nine days post-withdrawal of differentiation medium, PILCs on CS plated showed 1.2–2 ng/μg of protein, higher than those on regular plates (0.7–1.5 ng/μg of protein). Together

this suggested that CS improved the potential of porcine ADSCs to differentiate into pancreatic islet-like clusters, with improved functionality.

## 2.3 *Induced Pluripotent Stem Cells*

Induced pluripotent stem cells (iPSCs) are obtained by in vitro reprogramming of somatic cells to embryonic like pluripotent state, to be able to differentiate into multiple germ layers [35]. This makes them a great alternate to embryonic stem cells (ESCs). iPSCs can be generated from the tissue (skin or blood) of the same patient that will receive transplantation, without immune rejection. This leads to the development of personalized cell therapeutics for a broad array of diseases. Since their discovery in 2006, iPSCs have been used to generate various differentiated cell types, organoids to model diseases, etc. Till date iPSCs have been differentiated into pancreatic β-cells [36], cardiomyocytes [37], cholangiocytes [38], kidney organoids [39], lung organoids [40], cardiac organoids [41], etc. As the field of cellular therapeutics is evolving, strategies to improve the viability, functionality, and retention of cells post-transplantation gained importance. Tissue engineering strategies with biomaterials such as chitosan is one such approach. Therefore, here we focused on the studies that have used iPSCs and chitosan for regenerative applications.

Zhang et al. [42] have investigated whether ultrafine fibers' topography that mimic tendon extracellular matrix might induce tendon like differentiation of iPSC-MSCs. Ultrafine fibers (891 ± 71 nm) with 6 times more tensile strength and four-fold high Young's modulus more than random ones were prepared using SJES and CES techniques. Human iPSCs were differentiated into MSCs at 3-weeks confirmed by CD29, CD44, CD73, CD90, CD105 marker expression, adipo, osteo, and chondrogenic differentiation. Further $2 \times 10^4$ cells/cm$^2$ were seeded on ultrafine fiber scaffolds and cultured for 3 days. iPSC-MSCs cultured on aligned fibers showed increased expression of Mkx (tendon-related marker), and at day 14, increased mRNA levels of tendon-related genes SCX (two-fold), MKX (>ten-fold), HoxA11 (two-fold), Tnmd (two-fold), Epha4 and Bgn (>40-fold) Col1a1 (>50-fold) were observed compared to those on random fibers, in addition to decreased osteogenic differentiation (alizarin red) together confirming tenogenic differentiation of hiPSC-MSCs in vitro. Dil-labeled $14.5 \times 10^5$ hiPSC-MSCs/scaffold was transplanted into 6 mm wound created by removal of Achilles tendon in rats that were pre-treated for 24 h with cyclophosphamide. Anti-human nuclear staining showed viable cells at 2- and 4-week post-transplant with high degree of alignment along the axis of tensile load, better histology score, more collagen fiber deposition in the aligned fiber group, when compared to random fiber scaffold. Tendon ECM-related markers such as Col1a1, Col5a1, and Bgn were three-fold, five-fold, and six-fold increased 4-week post-align fiber transplant compared to random fibers. In addition, deposition of ColI and DCN, diameter of collagen fibers and stiffness were significantly higher in the aligned fiber group than the random

fiber scaffolds. Collectively this suggested ultrafine fiber induced differentiation and tendon regeneration by human iPSC-MSCs.

iPSCs from human gingival fibroblasts (hGFs) were generated by Ji et al. [43] and further tested their osteogenic differentiation potential using nanohydroxyapatite/chitosan/gelatin (HCG) scaffolds. hGFs were reprogrammed with Yamanaka factors and embryoid bodies (EBs) were generated, from which ESC like iPSC colonies were developed. Thus generated hiPSCs showed enhanced osteogenic differentiation (alizarin red) compared to hGFs. Composite scaffolds with different ratios of nHA particles, chitosan, and gelatin (HCG-111 and HCG-311) were prepared with different densities and characterized for phase separation, pore size, stiffness, adsorption, and compatibility with hiPSCs. HCG-111 showed larger pore width ($51.1 \pm 4.5$ μm), smoother pore walls (SEM), but HCG-311 had more nHA particles on the surface and showed more adsorption with α-MEM medium. 12-week post-culture, HCG-311 scaffold was filled with cells, ECM showed an increased bone-associated gene expression (OCN and OPN), lower expression of early markers (ALP and Col1) and was less degraded than the HCG-111. hiPSC-derived $1 \times 10^6$ Stro-1 positive cells were seeded onto $8 \times 5$ mm scaffolds and transplanted subcutaneously into nude mice after 1 week of incubation. Post-12-weeks, transplanted mice showed new bone formation, larger bone formation observed with HCG-311, with increased RUNX-2 and OCN expression compared to HCG-111 scaffolds, suggesting improved neobone regeneration with hiPSCs and HCG-311 scaffolds.

Worthington et al. [44] have used surfactant (DTAB and Brij 56) templated methacrylated chitosan hydrogels (MeCTS) for neuronal differentiation of iPSCs. Post fabrication, hydrogels were washed to remove the surfactants and incubated with pluripotency media for 24 h. Mouse fibroblast derived $2 \times 10^4$ iPSCs/well were seeded and tested for cytocompatibility. Cell attachment and growth was observed on non-templated and DTAB templated MeCTS hydrogels; however, Brij56 templated hydrogels did not support the growth of iPSCs. 1-week post-culture pluripotency markers Nanog, Oct4, Sox2, Lin28, Dnmt1, and Klf4 were expressed in iPSCs cultured on non-templated and DTAB templated hydrogels. Post-2 weeks, iPSCs expressed mRNA levels of neural retina markers Pax6, Otx2, and Rx and protein levels of neuronal differentiation marker Tuj-1 on non-templated and DTAB templated MeCTS hydrogels. Functionality of these cells cultured on MeCTS hydrogels needs to be determined.

Chitosan (CS) and chitosan-hyaluronic acid (CS/HA) membranes were prepared by Chang et al. [45] and their effect on the 3D spheroid formation, differentiation potential of human iPSCs (cell lines form cell bank, Tokyo) was studied and compared with that of vitronectin (VTN) substrates. At a cell density of $5 \times 10^4$ cells/mL, 90% of hiPSC spheroids of $<200$ μm diameter were formed on CS and CS-HA when cultured for 2–4 days. High alkaline phosphatase (AP) activity, increase in Oct4, Nanog, Tra1–60, SSEA4 was observed in the 3D spheroids on the CS membranes. EB formation, differentiation into ectodermal (Nestin), mesodermal (α-SMA), endodermal (GATA4) lineages were showed by both VTN and CS derived hiPSCs. Teratoma formation with ecto, meso, and endoderm layers was

observed 12-weeks post in NOD/SCID mice. RNA sequencing data showed that relative to VTN-derived, the CS-derived iPSCs showed differential expression of 400 genes (DEGs), with 243 upregulated and 189 downregulated genes. The DEGs were related to response to metal ions, hypoxia, might be due to 3D spheroid formation. An increase in naive marker genes was observed when cultured on CS and CS-HA membranes, however pluripotent markers Oct4, Sox2 and Sall4 did not change significantly. When passaged, the hiPSC-3D spheroids survived up to 100 passages, with high AP activity and pluripotency markers and germ layer differentiation potential. When BMP and TGFβ signaling were inhibited, hiPSC-3D spheroids showed neural stem cell like phenotype (Sox9, Pax6, Msi1, Sox2, and Nestin). When modulated with Wnt signaling for a week, beating cardiomyocyte-like spheroids were observed after 2 weeks, with cardiomyocyte marker (Actn2, Tnnc1, and Tnnt2) gene expression and cardiac troponin T (cTnT) at 3 and or 15-weeks post-differentiation. hiPSC-3D spheroids when induced on CS membranes showed hepatocyte differentiation (Alb, Cyp3a4, Ugt1a1) with albumin and E-cadherin expression at 20 days. This data suggests that CS membranes are a promising alternate to maintain and differentiate hiPSCs in 3D spheroid form, better than the conventional VTN substrates.

## *2.4 Stem Cell-Derived Extracellular Vesicles*

Extracellular vesicles (EVs) or previously known as exosomes are released by cells as an inter-cellular communication network that carries information in the form of proteins, lipids, nucleic acids (RNA, DNA), etc. [46]. Based on the type and state of the cells, these signals could be regenerative, destructive, immunomodulatory, etc. Stem cell-derived EVs seem to be more interesting with respect to the regenerative property and paracrine signaling of stem cells, such as MSCs. Their small size (50–200 nm) and non-immunogenic properties make the EV therapeutics a promising alternate to cellular therapeutics. However, challenges remain in clinical grade and scale of EV production from stem cells, route of delivery of EVs due to their short life span, etc.

Chitosan is widely studied for its drug delivery. In the study by Tao et al. [47] MSCs were isolated from the Synovium (SMSCs) and miR-126-3p was overexpressed, exosomes were obtained and were incorporated in chitosan hydrogel tested for their potential to repair cutaneous wounds. SMSCs were positive for CD73, CD44 and negative for CD34, CD45 and were able to differentiate into osteo, chondro, and adipocytes. 48 h SMSC conditioned media was subjected to ultracentrifugation and filtration to obtain EVs that were 30–150 nm and positive for Alix, Tsg101, CD9, CD63, and CD81 markers. miR-126 was overexpressed in SMSCs using lentivirus, and exosomes were isolated from these cells and incorporated into chitosan hydrogel and freeze dried to remove water (CS-SMSC-126-Exo) and characterized in comparison to CS hydrogel alone. Both hydrogels exhibited some weight loss during preparation, CS-SMSC-126-Exo showed higher

exothermic peaks, 10 μm macropores, nanoparticles of CS and C, O, and H according to SEM and EDS data. Immersion of CS-SMSC-126-Exo for 6 days in media showed a total of $183.08 \pm 15.44 \times 10^8$ exosome particles (ExoELISA) and Dil labeling also confirmed the release and presence of exosomes in perinuclear region of HMEC-1. Increase in miR-126 was confirmed by qRT-PCR in the SMSC-126-Exo. When added to HMEC1, SMSC-126-Exo increased the proliferation, migration, and tube formation potential of HMEC-1 cells and activated AKT and ERK1/2 pathways. In in vivo, CS-SMSC-126-Exo transplanted wounds were closed significantly faster by day 3, 7, and 14 with better healing than the controls. A significantly increased blood vessel number was observed in CS-SMSC-126-Exo transplanted wounds at day14 as observed with micro-CT. Further histological scoring confirmed re-epithelialization, thicker and mature granulation tissue, collagen deposition, development of hair follicles and sebaceous glands with CS-SMSC-126-Exo treated group. More number of newly formed vessels were identified with CD31 and α-SMA co-staining in CS-SMSC-126-Exo group at day 7 and day 14 in comparison to CS alone and non-treated groups. This study suggests that incorporation of miR-126 overexpressing SMSC-exosomes could be regenerative post-encapsulation into CS hydrogel and is a promising delivery method for EV therapeutics.

## 3 Summary and Future Perspectives

The goal of this review is to bring together the knowledge on different forms of chitosan and its interaction with multiple stem cell types such as adipose-derived MSCs, bone marrow-derived MSCs, induced pluripotent stem cells (Table 1). Successful regeneration and long-term functional recovery of tissue engineering constructs depends largely on their biocompatibility, stability, long-term integrity, and functionality, which in turn is influenced by the affinity between biomaterial and cells. As discussed in this review chitosan (CS) has been used in the form of hydrogel, scaffold either alone or in combination such as hydroxyapatite, collagen, gelatin, silk fibroin, etc. Studies that focused on the use of stem cells with chitosan largely focused on bone regeneration, myocardial infarct repair, and wound healing (Fig. 2). With the same type of CS hydrogel, three different cell types, AD-MSCs, BM-MSCs, and WJ-MSCs showed distinct osteogenic potential [27]. Especially with complex chemistry, the composite scaffold has broader properties, which need to be often tested with multiple cell types to identify a most compatible-functional cell type. Components such as cellular signaling modulating growth factors, cytokines, chemokines could be incorporated to enhance the endogenous stem or somatic cell stimulation, for example, like VEGF to stimulate endothelialization. Most of the studies focused on achieving recovery or successful repair of damage; however, more insight into mechanism of recovery, whether mediated by chemical or physical properties of hydrogels/scaffolds could provide better understanding of the materials' potential. This knowledge could be extrapolated to other models of

**Table 1** Table showing different reports that have used chitosan and AD-MSCs, BM-MSCs, and iPSCs for regenerative application

| References | Stem cell type | Stem cell source | Stem cell characterization | Modification of cells | Hydrogel/scaffold type | Application | Species tested | Model |
|---|---|---|---|---|---|---|---|---|
| [28] | BM-MSCs | Rat | CD29, CD45 | NA | Collagen-chitosan porous scaffold | Neuropathological repair | Rat | Traumatic brain injury |
| [27] | BM-MSCs | Human | Characterized previously | NA | Chitosan/hydroxyapatite/PCL | Bone regeneration | Rat | Bone defect model-tibia |
| [29] | BM-MSCs | Rat | Characterized previously | NA | Ferrite NP incorporated hydroxyapatite/chitosan (HA/CS) scaffold | Bone regeneration | Rat | Bone calvarial defect model |
| [30] | BM-MSCs | Mouse | Characterized previously | Transgenic mice expressing luciferase and GFP | Chitosan hydrogel | Cardiac regeneration | Mouse | Myocardial Infraction |
| [31] | AD-MSCs | Human | Characterized previously | Lentiviral eGFP | Silk-fibroin-chitosan scaffold | Wound repair | Mouse | Cutaneous wound |
| [32] | AD-MSCs | Rat | CD31, CD45, CD90, CD29; alizarin red, oil red O staining | Lentiviral firefly-luciferase and mRFP | Chitosan hydrogel | Cardiac regeneration | Rat | Myocardial Infraction |
| [32] | AD-MSCs | Human | CD31, CD45, CD90, CD29; alizarin red, oil red O staining | NA | Chitosan coated plates | Stemness maintenance | In vitro only | |
| [34] | AD-MSCs | Porcine | CD29, CD44 positive, tri-lineage differentiation | NA | Chitosan coated plates | Insulin secretion | In vitro only | |
| [42] | iPSC-MSCs | Human | Nanog, Oct4, SSEA4; CD31, CD45, CD90, CD29; alizarin red, oil red O staining etc. | NA | Chitosan-based ultrafine fibers | Tendon regeneration | Rat | Achilles tendon defect |

| | | | | | | | | |
|---|---|---|---|---|---|---|---|---|
| [43] | iPSCs | Human | Characterized previously | NA | Nanohydroxyapatite/ chitosan/gelatin scaffolds | Osteogenic differentiation | Mouse | Nude mice |
| [44] | iPSCs | Mouse | Characterized previously | NA | Surfactant templated chitosan hydrogel | Neuronal differentiation | In vitro only | |
| [45] | iPSCs | Human | Characterized previously | NA | Chitosan hyaluronic acid membranes | 3D culture, neuronal, hepatocyte, and cardiomyocyte differentiation | In vitro only | |

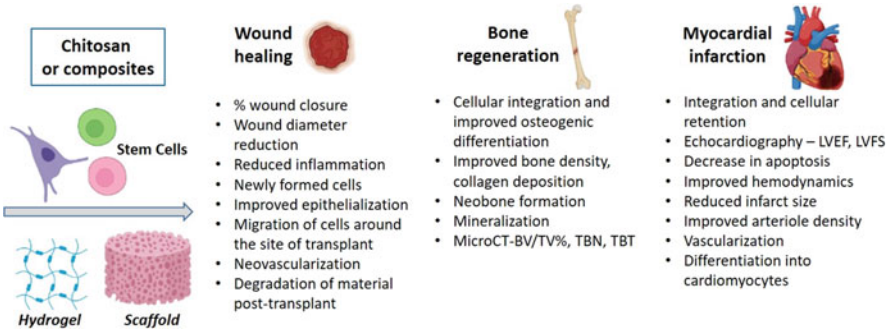


**Fig. 2** Schematic showing regenerative end points that were considered with chitosan-based materials in different models of wound healing, bone regeneration, and myocardial infarction. Made with Biorender.com

regeneration. Liu et al. [32] have used myocardial infarct model and suggested that CS might have a recovery effect on ROS laden microenvironment. ROS is one of the major consequences in normal tissues when exposed to radiation. Therefore, ROS scavengers, mitigators are of great interest for tissue regeneration post-radiation damage. CS and other biomaterials with such properties need to be studied using radiation models to get better insight into their potential.

In addition to stem cells, stem cell-derived products such as exosomes, 3D organoids could be more tested for regenerative application, for instance, by incorporating into hydrogels or scaffolds. EV therapeutics is currently an accelerating field and seem to hold great future in regenerative medicine. Storage of EVs is more challenging and studies that could investigate freeze-drying or lyophilization of EV incorporated hydrogels might solve the problem of storage, delivery, and in vivo sustained release of EVs.

Though we could not cover all the studies within the scope of this review, there are many interesting studies with acellular composite CS scaffolds in various small and large animal models of diseases.

## References

1. Yang TL (2011) Chitin-based materials in tissue engineering: Applications in soft tissue and epithelial organ. Int J Mol Sci:1936–1963
2. Deepthi S, Venkatesan J, Kim SK, Bumgardner JD, Jayakumar R (2016) An overview of chitin or chitosan/nano ceramic composite scaffolds for bone tissue engineering. Int J Biol Macromol 93:1338–1353
3. Anitha A, Sreeranganathan M, Chennazhi KP, Lakshmanan VK, Jayakumar R (2019) Corrigendum to "In vitro combinatorial anticancer effects of 5-fluorouracil and curcumin loaded N, O-carboxymethyl chitosan nanoparticles toward colon cancer and in vivo pharmacokinetic studies" (European Journal of Pharmaceutics and Biopharmaceutics (2014) 88(1) (238–251), (S0939641114001349), (10.1016/j.ejpb.2014.04.017)). Eur J Pharm Biopharm:44–46

4. Jayakumar R, Prabaharan M, Sudheesh Kumar PT, Nair SV, Tamura H (2011) Biomaterials based on chitin and chitosan in wound dressing applications. Biotechnol Adv:322–337
5. Mohan K, Ganesan AR, Muralisankar T, Jayakumar R, Sathishkumar P, Uthayakumar V et al (2020) Recent insights into the extraction, characterization, and bioactivities of chitin and chitosan from insects. Trends Food Sci Technol:17–42
6. Hsiao YC, Chen CN, Chen YT, Yang TL (2013) Controlling branching structure formation of the salivary gland by the degree of chitosan deacetylation. Acta Biomater 9:8214–8223
7. Ojeda-Hernández DD, Canales-Aguirre AA, Matias-Guiu J, Gomez-Pinedo U, Mateos-Díaz JC (2020) Potential of chitosan and its derivatives for biomedical applications in the central nervous system. Front Bioeng Biotechnol Front Media
8. Elbi S, Nimal TR, Rajan VK, Baranwal G, Biswas R, Jayakumar R et al (2017) Fucoidan coated ciprofloxacin loaded chitosan nanoparticles for the treatment of intracellular and biofilm infections of Salmonella. Coll Surf B Biointerf 160:40–47
9. Sandhya M, Aparna V, Maneesha KS, Raja B, Jayakumar R, Sathianarayanan S (2018) Amphotericin B loaded sulfonated chitosan nanoparticles for targeting macrophages to treat intracellular Candida glabrata infections. Int J Biol Macromol 110:133–139
10. Prabaharan M, Sivashankari PR (2015) Prospects of bioactive chitosan-based scaffolds in tissue engineering and regenerative medicine. Chitin Chitosan Regen Med:41–59
11. Patil SV, Nanduri LSY (2017) Interaction of chitin/chitosan with salivary and other epithelial cells – an overview. Int J Biol Macromol:1398–1406
12. Mohandas A, Deepthi S, Biswas R, Jayakumar R (2018) Chitosan based metallic nanocomposite scaffolds as antimicrobial wound dressings. Bioact Mater:267–277
13. Rajitha P, Gopinath D, Biswas R, Sabitha M, Jayakumar R (2016) Chitosan nanoparticles in drug therapy of infectious and inflammatory diseases. Expert Opin Drug Deliv:1177–1194
14. Gomathysankar S, Halim AS, Yaacob NS (2014) Proliferation of keratinocytes induced by adipose-derived stem cells on a chitosan scaffold and its role in wound healing, a review. Arch Plast Surg:452–457
15. Azuma K, Izumi R, Osaki T, Ifuku S, Morimoto M, Saimoto H et al (2015) Chitin, chitosan, and its derivatives for wound healing: old and new materials. J Funct Biomater 6:104–142
16. Zhang Y, Jiang X, Ren L (2019) Optimization of the adipose-derived mesenchymal stem cell delivery time for radiation-induced lung fibrosis treatment in rats. Sci Rep 9:1–10. https://doi.org/10.1038/s41598-019-41576-5
17. Kumar RA, Sivashanmugam A, Deepthi S, Iseki S, Chennazhi KP, Nair SV, et al. (2015) Injectable chitin-poly(#-Caprolactone)/Nano hydroxyapatite composite microgels prepared by simple regeneration technique for bone tissue engineering [internet]. http://pubs.acs.org
18. Bushkalova R, Farno M, Tenailleau C, Duployer B, Cussac D, Parini A et al (2019) Alginate-chitosan PEC scaffolds: a useful tool for soft tissues cell therapy. Int J Pharm:571
19. Miyajima H, Matsumoto T, Sakai T, Yamaguchi S, An SH, Abe M et al (2011) Hydrogel-based biomimetic environment for in vitro modulation of branching morphogenesis. Biomaterials 32:6754–6763
20. Ikemoto S, Mochizuki M, Yamada M, Takeda A, Uchinuma E, Yamashina S et al (2006) Laminin peptide-conjugated chitosan membrane: application for keratinocyte delivery in wounded skin. J Biomed Mater Res Part A 79:716–722
21. Shen Y, Jiang X, Meng L, Xia C, Zhang L, Xin Y (2018) Transplantation of bone marrow mesenchymal stem cells prevents radiation-induced artery injury by suppressing oxidative stress and inflammation. Oxidative Med Cell Longev 2018
22. Revi D, Paul W, Anilkumar TV, Sharma CP (2014) Chitosan scaffold co-cultured with keratinocyte and fibroblast heals full thickness skin wounds in rabbit. J Biomed Mater Res Part A 102:3273–3281
23. Vllasaliu D, Casettari L, Fowler R, Exposito-Harris R, Garnett M, Illum L et al (2012) Absorption-promoting effects of chitosan in airway and intestinal cell lines: a comparative study. Int J Pharm 430:151–160

24. Muanprasat C, Wongkrasant P, Satitsri S, Moonwiriyakit A, Pongkorpsakol P, Mattaveewong T et al (2015) Activation of AMPK by chitosan oligosaccharide in intestinal epithelial cells: Mechanism of action and potential applications in intestinal disorders. Biochem Pharmacol 96:225–236
25. Dominici M, Le Blanc K, Mueller I, Slaper-Cortenbach I, Marini FC, Krause DS et al (2006) Minimal criteria for defining multipotent mesenchymal stromal cells. Int Soc Cell Ther Position Statement Cytother 8:315–317
26. Martin I, Galipeau J, Kessler C, Le Blanc K, Dazzi F (2019) Challenges for mesenchymal stromal cell therapies. Sci Trans Med:11
27. Midha S, Jain KG, Bhaskar N, Kaur A, Rawat S, Giri S et al (2020) Tissue-specific mesenchymal stem cell-dependent osteogenesis in highly porous chitosan-based bone analogs. Stem Cells Transl Med
28. Yan F, Li M, Zhang HQ, Li GL, Hua Y, Shen Y et al (2019) Collagen-chitosan scaffold impregnated with bone marrow mesenchymal stem cells for treatment of traumatic brain injury. Neural Regen Res 14:1780–1786
29. Wang Q, Tang Y, Ke Q, Ke Q, Yin W, Zhang C et al (2020) Magnetic lanthanum-doped hydroxyapatite/chitosan scaffolds with endogenous stem cell-recruiting and immunomodulatory properties for bone regeneration. J Mater Chem B 8:5280–5292
30. Liu Y, Li P, Qiao C, Wu T, Sun X, Wen M, Zhang W (2020) Chitosan hydrogel enhances the therapeutic efficacy of bone marrow-derived mesenchymal stem cells for myocardial infarction by alleviating vascular endothelial cell pyroptosis. J Cardiovasc Pharmacol 75(1):75–83. https://doi.org/10.1097/FJC.0000000000000760
31. Altman AM, Yan Y, Matthias N, Bai X, Rios C, Mathur AB et al (2009) IFATS collection: human adipose-derived stem cells seeded on a silk fibroin-chitosan scaffold enhance wound repair in a murine soft tissue injury model. Stem Cells 27:250–258
32. Liu Z, Wang H, Wang Y, Lin Q, Yao A, Cao F et al (2012) The influence of chitosan hydrogel on stem cell engraftment, survival and homing in the ischemic myocardial microenvironment. Biomaterials 33:3093–3106
33. Cheng NC, Wang S, Young TH (2012) The influence of spheroid formation of human adipose-derived stem cells on chitosan films on stemness and differentiation capabilities. Biomaterials 33:1748–1758
34. Liu HY, Chen CC, Lin YY, Chen YJ, Liu BH, Wong SC et al (2017) Chitosan-assisted differentiation of porcine adipose tissue-derived stem cells into glucose-responsive insulin-secreting clusters. PLoS One 12
35. Takahashi K, Tanabe K, Ohnuki M, Narita M, Ichisaka T, Tomoda K et al (2007) Induction of pluripotent stem cells from adult human fibroblasts by defined factors. Cell 131:861–872
36. Pagliuca FW, Millman JR, Gürtler M, Segel M, Van Dervort A, Ryu JH et al (2014) Generation of functional human pancreatic β cells in vitro. Cell
37. Ronaldson-Bouchard K, Ma SP, Yeager K, Chen T, Song LJ, Sirabella D et al (2018) Advanced maturation of human cardiac tissue grown from pluripotent stem cells. Nature
38. Ogawa M, Ogawa S, Bear CE, Ahmadi S, Chin S, Li B et al (2015) Directed differentiation of cholangiocytes from human pluripotent stem cells. Nat Biotechnol 33:853–861
39. Takasato M, Er PX, Chiu HS, Maier B, Baillie GJ, Ferguson C et al (2015) Kidney organoids from human iPS cells contain multiple lineages and model human nephrogenesis. Nature 526:564–568
40. Jacob A, Morley M, Hawkins F, McCauley KB, Jean JC, Heins H et al (2017) Differentiation of human pluripotent stem cells into functional lung alveolar epithelial cells. Cell Stem Cell 21:472–488.e10
41. Voges HK, Mills RJ, Elliott DA, Parton RG, Porrello ER, Hudson JE (2017) Development of a human cardiac organoid injury model reveals innate regenerative potential. Dev Company Biol 144:1118–1127
42. Zhang C, Yuan H, Liu H, Chen X, Lu P, Zhu T et al (2015) Well-aligned chitosan-based ultrafine fibers committed Teno-lineage differentiation of human induced pluripotent stem cells for Achilles tendon regeneration. Biomaterials 53:716–730

43. Ji J, Tong X, Huang X, Zhang J, Qin H, Hu Q (2016) Patient-derived human induced pluripotent stem cells from gingival fibroblasts composited with defined Nanohydroxyapatite/chitosan/gelatin porous scaffolds as potential bone graft substitutes. Stem Cells Trans Med 5:95–105. https://doi.org/10.5966/sctm.2015-0139
44. Worthington KS, Green BJ, Rethwisch M, Wiley LA, Tucker BA, Guymon CA et al (2016) Neuronal differentiation of induced pluripotent stem cells on surfactant templated chitosan hydrogels. Biomacromolecules 17:1684–1695
45. Chang P-H, Chao H-M, Chern E, Hsu S (2020) Chitosan 3D cell culture system promotes naïve-like features of human induced pluripotent stem cells: a novel tool to sustain pluripotency and facilitate differentiation. Biomaterials:120575
46. Witwer KW, van Balkom BWM, Bruno S, Choo A, Dominici M, Gimona M et al (2019) Defining mesenchymal stromal cell (MSC)-derived small extracellular vesicles for therapeutic applications. J Extracell Vesicles 8
47. Tao S-C, Guo S-C, Li M, Ke Q-F, Guo Y-P, Zhang C-Q (2017) Chitosan wound dressings incorporating exosomes derived from MicroRNA-126-overexpressing synovium mesenchymal stem cells provide sustained release of exosomes and heal full-thickness skin defects in a diabetic rat model. Stem Cells Trans Med 6:736–747